Propene Adsorption on Clean and Oxygen-Covered Au(111) and Au(100) Surfaces

Kent A. Davis and D. Wayne Goodman*

Department of Chemistry, Texas A&M University, P.O. Box 30012, College Station, Texas 77842-3012

Received: May 8, 2000; In Final Form: June 28, 2000

The adsorption of propene on Au(111) and Au(100) was investigated using temperature-programmed desorption (TPD) and high-resolution energy loss spectroscopy (HREELS). A desorption activation energy of 9.4 kcal/mol and very small shifts of the vibrational frequencies from their gas-phase values indicate that the interaction of propene with the surface is weak. Energy loss spectra suggest that propene adsorbs with its molecular plane tilted slightly with respect to the surface plane. Atomic oxygen, chemisorbed on the gold surfaces, was characterized using TPD and low-energy electron diffraction (LEED), and its reaction with propene investigated. Propene desorption from the oxygen-covered surface occurs at 150 K with a shoulder at 200 K. Only propene and its total oxidation products desorbed from a one monolayer (1 ML) oxygen-covered surface. At an oxygen coverage of ∼0.4 ML, the higher temperature propene desorption feature at 200 K was maximized. HREEL spectra of propene giving rise to the 200 K desorption feature show shifts in the intensities and frequencies of the $-CH_2$ related vibrational features. Small amounts of product with masses 56 and 58 amu were observed for propene adsorbed onto a 0.4 ML oxygen-covered surface.

I. Introduction

Propene oxide is an important chemical intermediate whose production directly from propene has been the focus of research for many years. Silver-based catalysts are currently used for the oxidation of ethene to ethene oxide, although the detailed mechanism is still a subject of debate. Ultrahigh vacuum studies of norbornene and styrene with oxygen on silver surfaces have shown that these molecules are also active for partial oxidation. One apparently key feature that ethene, norbornene, and stryrene have in common is the absence of a labile allylic hydrogen. While selectivity for ethene epoxidation over these silver catalysts is high (greater than 80%), the selectivity for propene oxidation is low (less than 5%).[1,2] This is apparently due to facile abstraction of methyl hydrogens leading to the production of CO_2 and H_2O.[3−6] Metals such as Pd and Pt lead to total combustion products although the mechanism by which these metals facilitate oxidation is distinctly different from Ag.[7−9]

Other catalysts have shown varying degrees of activity for propene partial oxidation, one of the most promising catalysts being Au supported on TiO_2.[10−14] Au clusters smaller than 4 nm dispersed on TiO_2 produce propene oxide with very high selectivity.[15] Very little is known, however, about the mechanism or the active site involved in the partial oxidation.

The goal of the current work is to explore the interaction of propene with clean and oxygen-covered bulk gold as a benchmark for further studies of the special catalytic properties of nanoclusters of Au for propene epoxidation. The adsorption characteristics and vibrational spectra of propene on two different gold crystal faces and the interaction of adsorbed propene with chemisorbed oxygen are investigated.

II. Experimental Section

The experiments were carried out in an ultrahigh vacuum chamber with a base pressure of 2×10^{-10} Torr. The chamber was equipped with reverse view optics for LEED (Physical Electronics), a single-pass cylindrical mirror analyzer (Physical Electronics) for Auger spectroscopy (AES), a mass analyzer (UTI) for temperature-programmed desorption (TPD) and residual gas analysis, and a LK-2000 spectrometer (LK Technologies) for high-resolution electron energy loss spectroscopy (HREELS).

The Au(111) and Au(100) samples (10 mm in diameter and 1.5 mm thick), mechanically polished using 0.05 μm alumina paste, were spot-welded at the base of a loop of tantalum wire (<0.8 mm diameter). The crystals were attached to copper leads, allowing the sample to be resistively heated to 1100 K and cooled to 90 K. Temperature measurements were made with a 5% Re/W-26% Re thermocouple spot-welded to the edge of the sample.

The Au single crystals were cleaned by successive cycles of Ar sputtering and annealing in a vacuum to 1000 K for several hours to fully remove carbon. Additional cleaning cycles were necessary to remove small amounts of oxygen (as detected by AES).

Adsorption of propene was via a leak valve attached to a short stainless steel dosing tube, the end of which was less than 1 mm away from the Au surfaces. Monolayer coverages of propene were achieved with a background pressure of 3×10^{-9} Torr for 10 s with the sample maintained at 120 K. This exposure was found to be equivalent to that obtained by backfilling the UHV chamber with 3×10^{-8} Torr of propene for 100 s. Chemisorption of oxygen was carried out by dosing atomic oxygen, produced by passing molecular oxygen over a glowing tungsten filament, onto the Au surface at 300 K. The oxygen doses in the following sections are defined in terms of the exposure of thermally activated oxygen.

A primary electron energy of 3 keV was used in all AES measurements. An incident energy of 6 eV was used for the HREELS measurements with a typical resolution of 10 meV at full-width half-maximum (fwhm) of the elastic peak. All spectra were recorded with the electron beam at 60° to the surface normal with specular reflection. TPD experiments were performed with a heating ramp of 4 K/s.

10.1021/jp001699y CCC: $19.00
Published on Web 08/10/2000

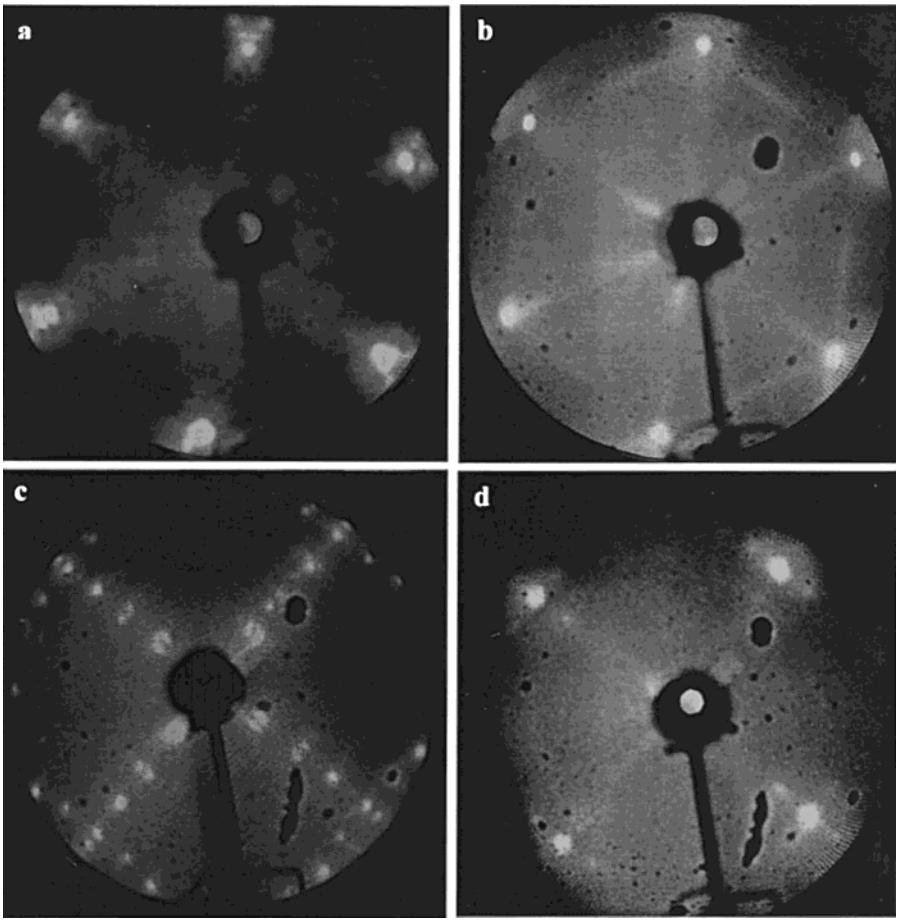

Figure 1. LEED photographs for (a) clean Au(111), (b) 0.5 ML oxygen on Au(111), (c) clean Au(100), and (d) 0.5 ML oxygen on Au(100).

III. Results and Discussion

In the following section, the synthesis of a chemisorbed oxygen layer and its characterization is first presented. The adsorption of propene on clean and oxygen-covered gold surfaces is then described.

A. Chemisorbed Oxygen. Previous studies have addressed the formation of an oxygen-covered gold surface. The evidence for oxygen chemisorption after dosing O_2 has been contradictory; however, recent work has shown that O_2 does not dissociatively adsorb on gold surfaces in the absence of an impurity such as calcium or silicon.[16−21] Chemisorbed oxygen has been studied by use of oxygen dc reactive sputtering,[22] by dosing O_2 across a hot filament,[21] by the decomposition of ozone on Au(111),[23] and the by reaction of N_2O_4 with ice on Au(111).[24]

In the experiments presented here, chemisorbed oxygen was formed by passing O_2 across a glowing filament, coiled near the opening of a stainless steel dosing tube. On a clean Au(111) or Au(100) surface after argon sputtering, AES data acquired before oxygen dosing or after a 10 min exposure to 5×10^{-8} Torr of O_2 in the absence of the hot filament showed no features corresponding to oxygen.

Figure 1a shows LEED images from clean Au(111) and a 0.5 monolayer (ML) thermally activated oxygen exposure to Au(111). The clean Au(111) surface undergoes a $(\sqrt{3} \times 22)$-rect reconstruction,[25] which splits the integral order spots. After an oxygen exposure corresponding to <0.1 ML of thermally activated oxygen at 300 K, the reconstruction is lifted and a sharp hexagonal pattern is observed. As the oxygen coverage is increased, the spots remain sharp with an increase in the background intensity until 0.5 ML of oxygen, at which point streaks connecting the first-order diffraction spots are apparent (Figure 1b). The background intensity and streaking increase from 0.5 to 1 ML oxygen; however the integral order spots remain sharp. As with the previous work of Koel et al., no (3×3)R30° LEED pattern was observed upon exposure of oxygen to Au(111) at elevated temperatures, in contrast to previous reports.[26−28]

The basic changes seen for Au(111) upon oxygen adsorption are seen as well for Au(100). The c(26×68) surface reconstruction leads to several additional spots between the integral order diffraction spots (Figure 1c), as has been reported.[25] This reconstruction is lifted with a very small coverage of oxygen (<0.1 ML). With an increase in oxygen coverage, this LEED pattern remains sharp with an increase in the diffuse background intensity and with streaking between the first-order spots (Figure 1d).

TPD data are shown in Figure 2a following the adsorption of thermally activated oxygen on Au(111). At low oxygen coverage the desorption maximum for O_2 is 505 K, increasing to 535 K at 0.5 ML. With an increase in the oxygen coverage above 0.5 ML, no further change in the peak desorption maximum is apparent. The inset of Figure 2 shows the ratio of the AES features associated with oxygen (514 eV) and gold (239 eV). The O(512 eV) to Au(239 eV) AES ratio increases linearly from 0 to a maximum of 1.5.

The desorption activation energy for oxygen from Au(111) using the Redhead approximation is 31 kcal/mol at 0.1 ML coverage, increasing to 34 kcal/mol at 0.5 ML. These values

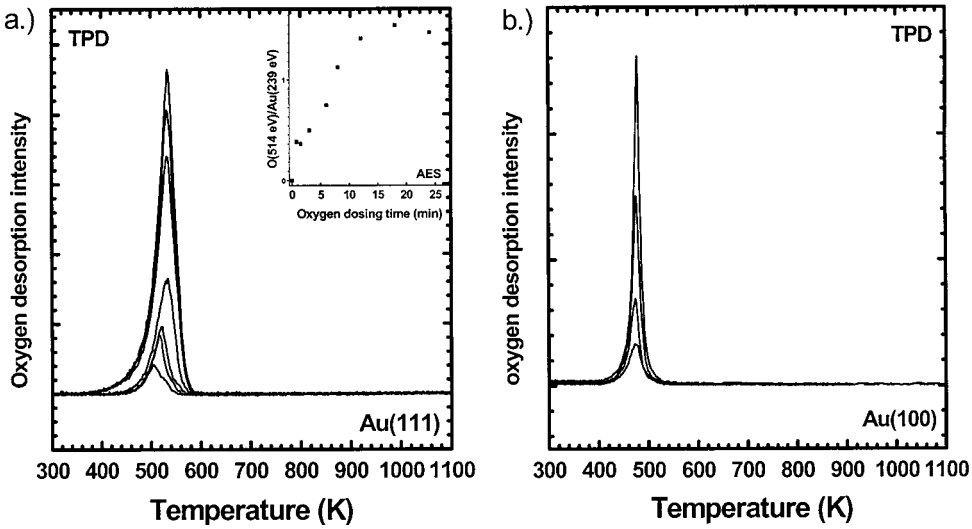

Figure 2. O_2 TPD for varying oxygen coverages on (a) Au(111) and (b) Au(100). The inset of (a) shows the change in the O/Au Auger ratio for increasing oxgyen coverage.

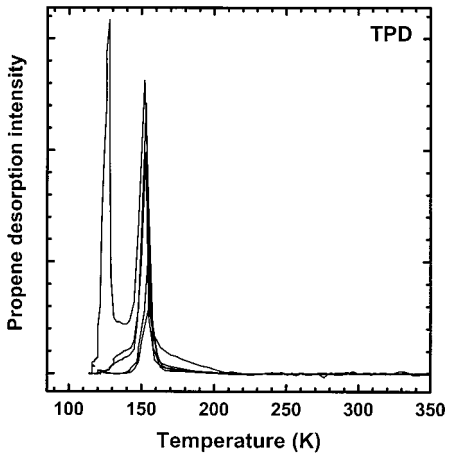

Figure 3. Temperature-programmed desorption spectra of propene on Au(111).

are identical to earlier work where oxygen exposures were carried out via ozone decomposition.[23]

Desorption spectra for oxygen chemisorbed on Au(100) are shown in Figure 2b. The width of the desorption feature (fwhm) is 30 K compared to 45 K for oxygen desorption from Au(111). In addition, the peak desorption maxima are at the same temperature (470 K) for all oxygen coverages. An estimate of the desorption activation energy using the Redhead approximation is 30 kcal/mol.

B. Propene/Au. *1. Propene Desorption.* TPD spectra of propene from Au(111) are shown in Figure 3 for several different propene exposures. With a 1 L exposure, the spectrum contains a single feature with a desorption maximum at 150 K corresponding to chemisorbed propene. Increases in propene exposure to 4 L lead to an increase in peak area and a slight shift of the peak maximum to 145 K. A shift to lower desorption temperatures with increasing coverage often indicates repulsive lateral interactions between adsorbate molecules. Similar results have been seen for propene adsorbed on Ag(110), where the temperature decrease of the desorption maximum was 15 K with an increase in coverage from 0.06 to 0.71 ML.[29]

In addition to enhancement of the primary desorption feature, a low-temperature shoulder appears at ca. 130 K for propene exposures >3 L. For a 20 L exposure, the 130 K feature saturates, and a second desorption feature, corresponding to desorption of three-dimensional (3D) solid propene layers, appears at 120 K.

For the Au(100) surface, propene desorbs (peak maximum at 140 K) at a slightly lower temperature than for Au(111) with a very similar desorption profile. For both surfaces, the only desorbing species are propene and small amounts of water and carbon monoxide. No significant accumulation of carbon was detectable via AES after multiple propene doses.

A Redhead analysis yields a desorption activation energy of 9.4 kcal/mol for propene on Au(111) and Au(100). This compares with 10.8−12.6 kcal/mol reported for propene from Ag(110) and 19 kcal/mol for propene from Pd(111).[29,30]

2. Adsorption Geometry. Propene, with C_s symmetry, has 21 normal modes, 14 of which have transition dipoles in the plane of symmetry containing the carbon atoms (a′) and 7 modes with transition dipoles perpendicular to this plane (a″). Propene most probably will interact with the gold substrate primarily via the π bond, in which case the molecular plane of symmetry will be parallel (or nearly so) to the surface plane. Assuming this geometry and taking into account the appropriate dipole selection rules (which allow strong excitation only of dynamic dipoles with components normal to the surface), only 7 vibrations, asymmetric with respect to the plane of symmetry in the gas phase (a″), should be observed. Some of these, however, may have weak intensities.

HREEL spectra of propene adsorbed on clean Au(111) at 100 K (Figure 4) contain five main features (assigned in Table 1) in addition to the elastic peak. The band assignments of Table 1 correlate directly with previous gas-phase assignments since none of the features deviates by more than 25 cm^{-1} from the gas-phase frequencies.[31,32] The feature at 920 cm^{-1} is the most intense feature in the adsorbed layer (as well as in the gas phase) and is assigned to be the $-CH_2$ wagging vibration. The next most intense feature is at 590 cm^{-1}, which corresponds to the $-CH_2$ twisting vibration. The $-CH_3$ asymmetric distortion vibration is apparent at 1430 cm^{-1} and a $-CH_3$ stretching vibration is observed at ca. 2960 cm^{-1}. The three remaining modes of a″ symmetry are expected to have low intensities and to be obscured by their proximity to the elastic peak and/or to the 920 cm^{-1} CH_2 wagging vibration.

In addition to the four bands discussed above, a weak loss feature at 1630 cm^{-1} is apparent and is assigned to the C═C stretching vibration. This band could be a consequence of a perpendicular dipole moment induced via interaction of the C═

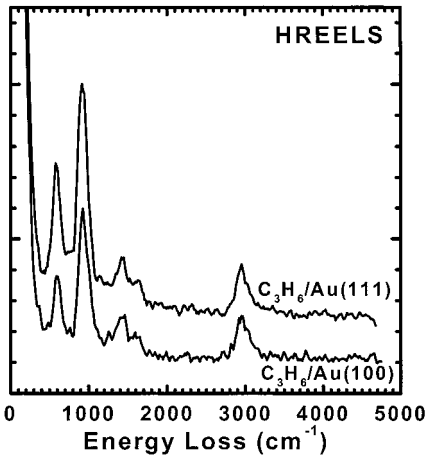

Figure 4. HREEL spectra of propene adsorbed on clean Au(111) and clean Au(100) at 100 K.

TABLE 1: Vibrational Frequencies of Selected Vibrational Modes of Propene in the Gas Phase and Adsorbed on Gold[a]

symmetry	assignment	gas-phase frequency[b]	adsorbed-phase frequency
a″	CH_3 asym stretch	2958	2960
	CH_3 asym deform	1433	1430
	CH_3 rock	1040	
	CH bend + CH_2 tw	988	
	CH_2 wag	908	920
	C−CH_2 twist	578	590
	C−CH_3 torsion	157	
a′	C═C stretch	1645	1630

[a] All values have units of cm^{-1}. [b] Reference 32.

C moiety with the surface, albeit a weak interaction, since such π−d interactions are known to strongly depend on the C═C distance from the surface.[33,34] However, the small (25 cm^{-1}) red shift of the π bonded C═C stretching frequency from the corresponding gas-phase frequency argues against this interpretation and favors the conclusion that the propene molecules are tilted with respect to the Au(111) surface. Ethene, acetylene, and propene also have been shown to adsorb with their π bonds slightly tilted with respect to the surface plane on Pt(111) and Ag(110).[34−36]

A tilted molecular plane should then lead to enhanced contributions of other a′-type modes in the HREELS. In particular the −CH_3 distortion/−CH_2 scissor modes near 1450 cm^{-1} and the five in-plane C−H stretching modes near 2950 cm^{-1}, coincident with the previously assigned out-of-plane vibrations, should be apparent. Comparison of the integrated loss feature of propene on Au with FTIR data of propene on Ag(110) and gas-phase propene provide additional information concerning the bond angle of propene with respect to the surface. The ratio of the integrated intensities of the −CH_2 wagging vibration (908 cm^{-1}) and the nearby less intense trans wagging mode (∼990 cm^{-1}) compared to the integrated intensity of the out-of-plane C−H stretching feature is 6.3 for gas-phase propene. This ratio is 6.0 for propene on Ag(110) where propene adsorbs nearly parallel to the surface.[29,35] For propene on Au(111), this ratio is 3.4, suggesting that tilting of the propene with respect to Au(111) leads to the observed enhancement of the C−H stretching modes in HREELS.

C. Propene/O/Au. *1. Temperature-Programmed Reaction.* TPD was used to study the interaction of propene with oxygen on the Au(111) and Au(100) surfaces. On a 1 ML oxygen-covered Au(111) surface, propene desorption is unchanged from the clean gold surface (Figure 5). The desorption peak, however,

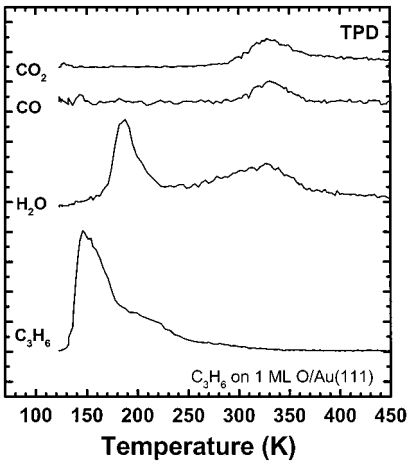

Figure 5. Propene (1 ML) desorption spectra on 1 ML oxygen-covered Au(111).

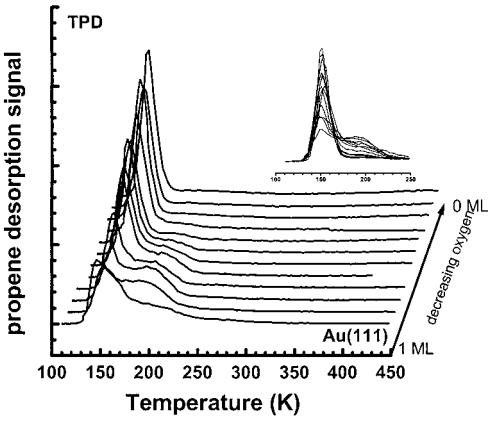

Figure 6. TPD spectra of propene on O/Au(111) offset for clarity. The inset shows the same spectra with neither *x* nor *y* offset.

is broadened substantially and a shoulder appears on the high-temperature side of the main desorption feature. In addition to propene desorption, water, carbon monoxide, and carbon dioxide desorb concertedly at ca. 330 K with no detectable (via AES) accumulation of carbon on the surface. No desorbing species were detected with masses 56 and 58, corresponding to partially oxidized propene, e.g. acrolein, propene oxide, or acetone.

It is evident from AES and TPD that residual oxygen remains following desorption of a 1 ML exposure of propene. Propene desorption as a function of decreasing oxygen coverage on Au(111) is shown in Figure 6. The lower spectrum corresponds to a 1 ML dose of propene following the formation of an oxygen layer and is identical to the propene desorption spectrum shown in Figure 5. Successive spectra were recorded following 1 ML propene exposures. The second propene desorption in the series differs from the first in that (i) the main physisorbed propene desorption feature decreases slightly in intensity and (ii) the shoulder at ∼200 K increases by nearly a factor of 2. Desorption spectra following the third exposure shows growth in the 150 K peak with essentially no change in the 200 K feature. Following additional 1 ML propene exposures, the spectra show increases in the intensity of the 150 K feature accompanied by decreases in the shoulder at 200 K. After eight successive exposures of propene, the 200 K shoulder disappears and the primary desorption feature is identical to that recorded for a 1 ML propene exposure to the clean Au(111) surface in Figure 3.

Essentially identical behavior for propene desorption is observed for the Au(100) surface (Figure 7). For Au(100),

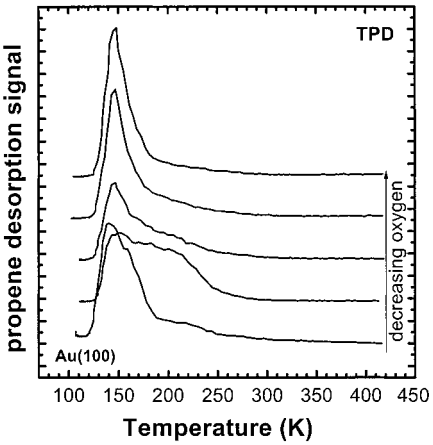

Figure 7. TPD spectra of propene on O/Au(100).

however, depletion of surface oxygen with propene exposure is more pronounced. For example, by the fifth propene exposure, the 200 K feature has vanished (compared with the eighth exposure for Au(111)). There is an increase in the total yield of oxidation products after the first propene exposure with a significant decrease in these products for subsequent exposures.

The invariance of the propene desorption temperature with oxygen coverage contrasts markedly with similar experiments of propene and propene oxide adsorbed on oxidized Ag(110), where the propene desorption temperature increased as much as a 50 K with an increase in oxygen coverage from 0 to 0.3 ML.[6,37]

Experiments with initial oxygen coverages less than 1 ML were also performed. The reproducibility of oxygen dosing at these lower coverages varied; however, generally these data were consistent with the results for the intermediate oxygen coverages shown in Figure 6. The maximum yield of the 200 K desorption species occurs at an oxygen coverage of ~0.4 ML.

It is also noteworthy that the yield of the total oxidation species decreases markedly following the first propene dose. The second spectrum in the series of Figure 6, for example, shows approximately half as much H_2O, CO_2, and CO as the first exposure. By the fourth propene exposure for Au(111) or the second dose for Au(100), these products are essentially nonexistent.

For oxygen coverages below 0.5 ML on Au(111), limited amounts of masses 56 and 58 desorbed. Desorption of mass 56 was also observed from Au(100) at similar oxygen coverages; however, no mass 58 was found for this surface. Mass 56 and 58 TPD data following propene adsorption from ~0.5 ML oxygen-covered Au(111) and Au(100) are shown in Figure 8. Masses 56 and 58 correspond to several possible partial oxidation products of propene including acrolein, propene oxide, and acetone. Further experiments to ascertain the identity of the partial oxidation species were not undertaken due to the relatively large number of possible similar species and their low production rate. Ancillary TPD experiments following the adsorption of propene oxide on Au(111) allowed the yield of propene oxide to be estimated at approximately 2% of a monolayer, assuming that the mass 58 species is indeed propene oxide.

The apparent differences in the reactivity of oxygen on the Au(111) and Au(100) surfaces at this point is purely speculative; however, one obvious contribution could be the differences in the atomic roughnesses of these two surfaces, i.e., the more open (100) face being more reactive than the (111) surface. It has been observed for Ag(110) that oxygen adsorbs in long metal−oxygen chains and that its reactivity is greatest for terminal oxygens.[6] Oxygen adsorbed on Ag(110) at 150 K has been shown to have shorter chains and is more reactive for CO or propene oxidation than oxygen adsorbed at 190−250 K.[38] Similar differences in oxygen ordering on Au(111) and Au(100) could lead to an increase in the higher relative activity of the Au(100) surface. Au(111) has also been shown to exhibit metal−oxygen chains similar to Ag;[28] however, the chemisorbed oxygen structure for Au(100) has not been studied.

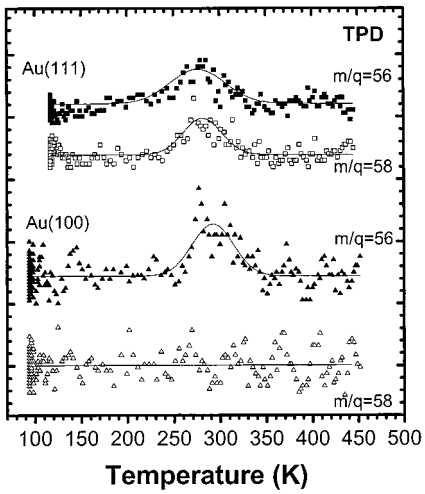

Figure 8. TPD spectra demonstrating typical production of mass 56 and 58 partial oxidation products for 1 ML propene on ~0.5 ML oxygenated Au(111) and Au(100).

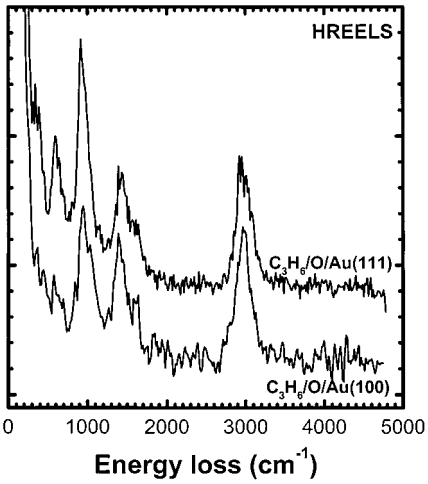

Figure 9. Energy loss spectra of propene adsorbed on oxygenated Au(111) and Au(100) surfaces.

2. High-Resolution Energy Loss Spectra. The HREEL spectra of propene adsorbed on oxygen-covered Au(100) and Au(111) at 100 K, shown in Figure 9, are not noticeably different from propene on the corresponding clean surfaces of Figure 4. The only apparent difference between the spectra of propene on Au, with and without oxygen, is the decrease in intensity for the two lowest frequency modes involving the $-CH_2$ moiety. The decrease in intensity of the $-CH_2$ modes is most significant for propene adsorbed on oxygen-covered Au(100) compared to the clean surface. For each, the C═C stretching vibration is clearly apparent with little change in intensity, suggesting little change in the adsorption bonding geometry. That the only change in the vibrational spectrum occurs at the double bond end of the molecule is logical considering the likelihood that the primary interaction of propene with Au will be via the π-bond. However, the lack of any measurable shift of the C═

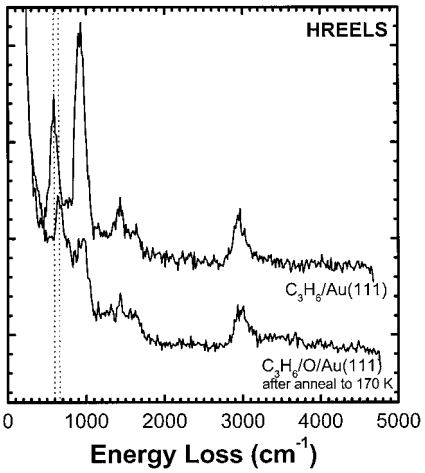

Figure 10. Comparison between HREEL spectra of propene on Au(111) and propene on O/Au(111) after anneal to 170 K.

C stretch mode appears to be inconsistent with this conclusion. If the decrease in intensity of the $-CH_2$ wag and torsion modes were due to an increase in the π-bond interaction with the surface, a shift of the C═C bond to lower energy should be a reasonable consequence. If, however, the more strongly bound propene molecules undergo a change in orientation so that their C═C bonds are more parallel to the surface, these molecules would not be detected and a shift may not be observed. In any case, these data do confirm that the interaction between propene and chemisorbed oxygen on gold is very weak.

After an anneal of propene adsorbed on oxygen-covered Au(111) and Au(100) to 170 K, the more weakly bound molecules desorb, leaving the more strongly bound ones (~200 K feature). The HREEL spectrum of this strongly bound species is shown in Figure 10 for an initial oxygen coverage of 0.4 ML on Au(111) with a reference spectrum of propene on the clean Au(111) surface. It is noteworthy that the intensities of the two lowest frequency modes change the most; however, importantly, the *frequency* of the lowest energy vibration is also altered. This mode, the $-CH_2$ torsion vibration, exhibits a blue shift of ~80 cm^{-1}. The frequency of the C═C stretching vibration remains constant at 1630 cm^{-1}. The continued appearance of this feature tends to discount the possibility that the strongly bound propene species has undergone an orientation change where its C═C bond is more parallel to the surface. This more tightly bound species may not be a precursor to propene oxide since a strong propene-oxygen interaction via the C═C moiety should give rise to C−O−C ring vibrations around 807 and 872 cm^{-1}, which are absent.[39]

IV. Conclusions

Propene adsorbs on clean gold surfaces very weakly, exhibiting a vibrational spectrum nearly identical to that of gas-phase propene. HREEL data indicate that the molecule bonds with its plane slightly tilted with respect to the surface plane and desorbs molecularly with an activation energy of 9.4 kcal/mol.

Propene adsorbs more tightly on an oxygen-covered gold surfaces, albeit with a weak propene−oxygen interaction, and reacts with oxygen at high coverages to produce CO_2, CO, and H_2O. HREELS reveals that the vibrational properties of propene on oxygen-covered Au is essentially the same as propene on clean Au except for perturbations of the $-CH_2$ torsion and wag modes that decrease their HREELS intensities. The presence of mass 56 and 58 desorption features indicates that partial oxidation of propene over gold can occur albeit in very small quantities for bulk gold surfaces. Clearly, the facile nature of the propene−oxygen reaction on Au clusters is a manifestation of the unique properties of nanosized Au catalysts.

Acknowledgment. This work was supported by the Department of Energy, the Office of Energy Research, Division of Chemical Sciences, the Robert A. Welch Foundation, and the Dow Chemical Co.

References and Notes

(1) Cant, N. W.; Hall, W. K. *J. Catal.* **1978**, *52*, 81.
(2) Akimoto, M.; Ichikawa, K.; Echigoya, E. *J. Catal.* **1982**, *76*, 333.
(3) Barteau, M. A.; Madix, R. J. *J. Am. Chem. Soc.* **1983**, *105*, 344.
(4) Roberts, J. T.; Madix, R. J.; Crew, W. W. *J. Catal.* **1993**, *141*, 300.
(5) Hu, Z.; Nakai, H.; Nakatsuji, H. *Surf. Sci.* **1998**, *401*, 371.
(6) Ranney, J.; Bare, S. *Surf. Sci.* **1997**, *382*, 266.
(7) Guo, X.-C.; Madix, R. J. *Surf. Sci.* **1997**, *391*, L1165.
(8) Guo, X.-C.; Madix, R. J. *J. Am. Chem. Soc.* **1995**, *117*, 5523.
(9) Gabelnick, A. M.; Gland, J. L. *Surf. Sci.* **1999**, *440*, 340.
(10) Adams, C. R.; Jennings, T. J. *J. Catal.* **1964**, *3*, 549.
(11) Grasselli, R. K.; Suresh, D. D. *J. Catal.* **1972**, *25*, 273.
(12) Burrington, J. D.; Kartisek, C. T.; Grasselli, R. K. *J. Catal.* **1981**, *69*, 495.
(13) Geenen, P.; Boss, H.; Pott, G. *J. Catal.* **1982**, *77*, 499.
(14) Schulz, K. H.; Cox, D. F. *Surf. Sci.* **1992**, *262*, 318.
(15) Hayashi, T.; Tanaka, K.; Haruta, M. *J. Catal.* **1998**, *178*, 566.
(16) Chesters, M. A.; Somorjai, G. A. *Surf. Sci.* **1975**, *52*, 21.
(17) Schrader, M. E. *Surf. Sci.* **1978**, *78*, L227.
(18) Eley, D. D.; Moore, P. B. *Surf. Sci.* **1978**, *76*, L599.
(19) Legaré, P.; Hilaire, L.; Sotto, M.; Maire, G. *Surf. Sci.* **1980**, *91*, 175.
(20) Pireaux, J. J.; Chtaïb, M.; Delrue, J. P.; Thiry, P. A.; Liehr, M.; Caudano, R. *Surf. Sci.* **1984**, *141*, 211.
(21) Canning, N. D. S.; Outka, D.; Madix, R. J. *Surf. Sci.* **1984**, *141*, 240.
(22) Pireaux, J. J.; Liehr, M.; Thiry, P. A.; Delrue, J. P.; Caudano, R. *Surf. Sci.* **1984**, *141*, 221.
(23) Saliba, N.; Parker, D. H.; Koel, B. E. *Surf. Sci.* **1998**, *410*, 270.
(24) Wang, J.; Koel, B. E. *Surf. Sci.* **1999**, *436*, 15.
(25) Van Hove, M. A.; Koestner, R. J.; Stair, P. C.; Bibérian, J. P.; Kesmodel, L. L.; Bartoš, I.; Somorjai, G. A. *Surf. Sci.* **1981**, *103*, 189.
(26) Cao, J.; Wu, N.; Qi, S.; Feng, K.; Zei, M. S. *Chinese Phys. Lett.* **1989**, *6*, 92.
(27) Chevrier, J.; Huang, L.; Zeppenfeld, P.; Comsa, G. *Surf. Sci.* **1996**, *355*, 1.
(28) Huang, L.; Zeppenfeld, P.; Chevrier, J.; Comsa, G. *Surf. Sci.* **1996**, *352*−*354*, 285.
(29) Pawela-Crew, J.; Madix, R. J. *J. Chem. Phys.* **1996**, *104*, 1699.
(30) Thornburg, N. A.; Abdelrehim, I. M.; Land, D. P. *J. Phys. Chem.* **1999**, *103*, 8894.
(31) Lord, R. C.; Venkateswarlu, P. *J. Opt. Soc. Am.* **1953**, *43*, 1079.
(32) Radziszewski, J. G.; Downing, J. W.; Gudipati, M. S.; Balaji, V.; Thulstrup, E. W.; Michl, J. *J. Am. Chem. Soc.* **1996**, *118*, 10275.
(33) Lehwald, S.; Ibach, H. *Surf. Sci.* **1979**, *89*, 425.
(34) Demuth, J. E. *Surf. Sci.* **1979**, *84*, 315.
(35) Solomon, J. L.; Madix, R. J.; Stöhr, J. *J. Chem. Phys.* **1990**, *93*, 8379.
(36) Cassuto, A.; Mane, M.; Tourillon, G.; Parent, P.; Jupille, J. *Surf. Sci.* **1993**, *287*, 460.
(37) Ranney, J.; Gland, J.; Bare, S. *Surf. Sci.* **1998**, *401*, 1.
(38) Burghaus, U.; Conrad, H. *Surf. Sci.* **1996**, *352*, 201.
(39) Polavarapu, P. L.; Hess, B. A.; Schaad, L. J. *J. Chem. Phys.* **1985**, *82*, 1705.